

Tensor-product representations for string-net condensed states

Zheng-Cheng Gu,¹ Michael Levin,² Brian Swingle,¹ and Xiao-Gang Wen¹

¹*Department of Physics, Massachusetts Institute of Technology, Cambridge, Massachusetts 02139, USA*

²*Department of Physics, Harvard University, Cambridge, Massachusetts 02138, USA*

(Received 16 September 2008; published 23 February 2009)

We show that general string-net condensed states have a natural representation in terms of tensor product states (TPSs). These TPSs are built from local tensors. They can describe both states with short-range entanglement (such as the symmetry-breaking states) and states with long-range entanglement (such as string-net condensed states with topological/quantum order). The tensor product representation provides a kind of “mean-field” description for topologically ordered states and could be a powerful way to study quantum phase transitions between such states. As an attempt in this direction, we show that the constructed TPSs are fixed points under a certain wave-function renormalization-group transformation for quantum states.

DOI: [10.1103/PhysRevB.79.085118](https://doi.org/10.1103/PhysRevB.79.085118)

PACS number(s): 71.27.+a

I. INTRODUCTION

In modern condensed-matter theory, an essential problem is the classification of phases of matter and the associated phase transitions. Long-range correlation and broken symmetry¹ provide the conceptual foundation to the traditional theory of phases. The mathematical description of such a theory is realized very naturally in terms of order parameters and group theory. The Landau symmetry-breaking theory was so successful that people started to believe that the symmetry-breaking theory described all phases and phase transitions. From this point of view, the discovery of the fractional quantum Hall (FQH) effect² in the 1980s appears even more astonishing than what we realized. These unique phases of matter have taught us a very important lesson: when quantum effects dominate, entirely new kinds of order, orders not associated with any symmetry, are possible.³ Similarly, new type of quantum phase transitions, such as the continuous phase transitions between states with the same symmetry^{4–7} and incompatible symmetries^{8,9} are possible. There is literally a whole new world of quantum phases and phase transitions waiting to be explored. The conventional approaches, such as symmetry breaking and order parameters, simply do not apply here.

The particular kind of order present in the fractional quantum Hall effect is known as topological order,³ or more specifically, chiral topological order because of broken parity and time-reversal (PT) symmetry. Topological phases which preserve parity and time-reversal symmetry are also possible^{7,10–19} and we will focus on these phases in this paper. An appealing physical picture has recently been proposed for this large class of PT symmetric topological phases in which the relevant degrees of freedom are stringlike objects called string nets.^{20,21} Just as particle condensation provides a physical picture for many symmetry-breaking phases, the physics of highly fluctuation strings, string-net condensation, has been found to underlie PT symmetric topological phases.

The physical picture of string-net condensation provides also a natural mathematical framework, tensor category theory, which can be used to write down fixed-point wave functions and calculate topological quantum numbers.^{21,22}

These topological quantum numbers include the ground-state degeneracy on a torus, the statistics and braiding properties of quasiparticles, and topological entanglement entropy.^{23,24} All these physical properties are quite nonlocal, but they can be studied in a unified and elegant manner using the nonlocal string-net basis.

Unfortunately, this stringy picture for the physics underlying the topological phase seems poorly suited for describing phase transitions out of the topological phase. The large and nonlocal string-net basis is difficult to deal with in the low energy continuum limit appropriate to a phase transition. Trouble arises from our inability to do mean-field theory to capture the stringiness of the state in an average local way. Indeed, the usual tool box built around the local order parameters is no longer available since there is no broken symmetry. We are thus naturally led to look for a local description of topological phases which lack traditional order parameters.

Remarkably, there is already a promising candidate for such a local description. A new local ansatz, tensor product states (also called projected entangled pair states), has recently been proposed for a large class of quantum states in dimensions greater than 1.²⁵ In the tensor product state (TPS) construction and its generalizations,^{26,27} the wave function is represented by a local network of tensors giving an efficient description of the state in terms of a small number of variables.

The TPS construction naturally generalizes the matrix product states in one dimension.^{28,29} The matrix product state formulation underlies the tremendous success of the density-matrix renormalization group for one-dimensional systems.³⁰ The TPS construction is useful for us because it allows one to locally represent the patterns of long-range quantum entanglement^{23,24,31} that lies at the heart of topological order. In this paper, we show that the general string-net condensed states constructed in Ref. 21 have natural TPS representations. Thus the long-range quantum entanglement in a general (nonchiral) topologically ordered state can be captured by TPS. The local tensors that characterize the topological order can be viewed as the analog of the local order parameter describing symmetry-breaking order.

In addition to our basic construction, we demonstrate a set of invariance properties possessed by the TPS representation

of string-net states. These invariance properties are characteristic of fixed-point states in a new renormalization group for quantum states called the tensor entanglement renormalization group (TERG).³² This fixed-point property of string-net states has already been anticipated²¹ and provides a concrete demonstration of string-net states as the infrared fixed points of PT symmetric topological phases.

We would like to point out that the string-net states can also be represented in terms of the multiscale entanglement renormalization ansatz (MERA),^{26,27} where the ansatz does not flow at each scale.³³ In other words, MERA (Refs. 26 and 27) represents a different way to do renormalization on the wave function. The string-net wave functions are also fixed-point wave functions under such a wave-function renormalization procedure.

To compare the two renormalization pictures, we like to point out that, under the MERA approach, the string-net wave functions are rewritten in term of a treelike tensor network in three dimensions (3D), where each level of the tree forms a two-dimensional (2D) tensor network and different levels represent different coarse-graining scales. The fixed-point or the scale-invariant nature of string-net states is captured by the fact that the tensors at each level of the tree are the same. On the other hand, under the TERG approach, we show that the tensor network that give rise to the norm of the string-net wave function is invariant under coarse graining.

This paper is organized as follows. In Secs. II and III we construct TPS representations for the two simplest string-net condensed states. In Sec. IV we present the general construction. In Sec. V, we use the TPS representation to show that the string-net condensed states are fixed points of the tensor entanglement renormalization group. Most of the mathematical details can be found in the appendix.

II. Z_2 GAUGE MODEL

We first explain our construction in the case of the simplest string-net model: Z_2 lattice gauge theory (also known as the toric code).^{17,18,20,21} In this model, the physical degrees of freedom are spin-1/2 moments living on the links of a square lattice. The Hamiltonian is

$$H = - \sum_p \prod_{i \in p} \sigma_i^x - \sum_v \prod_{i \in v} \sigma_i^z.$$

Here $\prod_{i \in p} \sigma_i^x$ is the product of the four σ_i^x around a square p and \sum_p is a sum over all the squares. The term $\prod_{i \in v} \sigma_i^z$ is the product of the four σ_i^z around a vertex v and \sum_v is a sum over all the vertices. The ground state $|\Psi_{Z_2}\rangle$ of H is known exactly. To understand this state in the string language, we interpret the $\sigma^z = -1$ and $\sigma^z = 1$ states on a single link as the presence or absence of a string. (This string is literally an electric flux line in the gauge theory.) The ground state is simply an equal superposition of all closed-string states (e.g., states with an even number of strings incident at each vertex)

$$|\Psi_{Z_2}\rangle = \sum_{X \text{ closed}} |X\rangle. \quad (1)$$

While this state is relatively simple, it contains nontrivial topological order. That is, it contains quasiparticle excita-

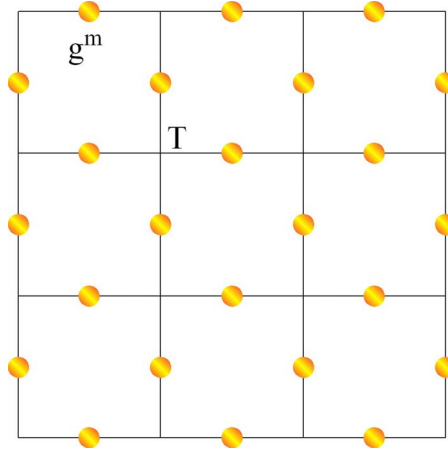


FIG. 1. (Color online) Z_2 gauge model on a square lattice. The dots represent the physical states which are labeled by m . The above graph can also be viewed as a tensor network, where each dot represents a rank-3 tensor g and each vertex represents a rank-4 tensor T . The two legs of a dot represent the α and β indices in the rank-3 tensor $g_{\alpha\beta}^m$. The four legs of a vertex represent the four internal indices in the rank-4 tensor $T_{\alpha\beta\gamma\lambda}$. The indices on the connected links are summed over which define the tensor trace tTr .

tions with nontrivial statistics (in this case, Fermi statistics and mutual semion statistics) and it exhibits long-range entanglement (as indicated by the nonzero topological entanglement entropy^{23,24}).

The above state has been studied before using TPS.^{27,34} Our TPS construction is different from earlier studies because it is derived naturally from the string-net picture. As illustrated in Fig. 1, we present two sets of tensors: T tensors living on the vertices and g tensors living on the links. The g tensors are rank 3 tensors $g_{\alpha\alpha'}^m$, with one physical index m running over the two possible spin states \uparrow, \downarrow and two “internal” indices α, α' running over some range $0, 1, \dots, k$. The T tensors are rank 4 tensors $T_{\alpha\beta\gamma\delta}$ with four internal indices $\alpha, \beta, \gamma, \delta$ running over $0, 1, \dots, k$.

In the TPS construction, we construct a quantum wave function for the spin system from the two tensors, T and g . The wave function is defined by

$$\Psi(\{m_i\}) = \text{tTr}[\otimes_v T \otimes_l g^{m_l}]. \quad (2)$$

To define the tensor trace (tTr), one can introduce a graphic representation of the tensors (see Fig. 1). Then tTr means summing over all unphysical indices on the connected links of tensor network.

It is easy to check that the Z_2 string-net condensed ground state that we discussed above is given by the following choice of tensors with internal indices α, β, \dots running over 0, 1:

$$T_{\alpha\beta\gamma\delta} = \begin{cases} 1 & \text{if } \alpha + \beta + \gamma + \delta \text{ even} \\ 0 & \text{if } \alpha + \beta + \gamma + \delta \text{ odd,} \end{cases} \quad (3)$$

$$g_{00}^\uparrow = 1, \quad g_{11}^\downarrow = 1, \quad \text{others} = 0, \quad (4)$$

The interpretation of these tensors is straightforward. The rank-3 tensor g behaves like a projector which essentially

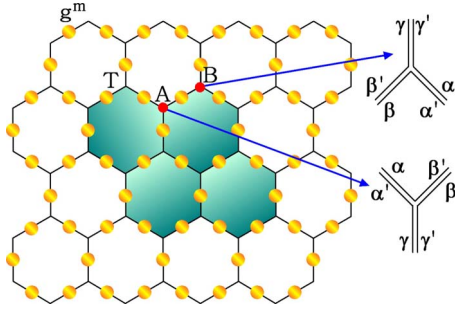


FIG. 2. (Color online) The double-semion model on the honeycomb lattice. The ground-state wave function (5) has a TPS representation given by the above tensor network. Note that T and g has a double line structure. Note that the vertices form a honeycomb lattice which can be divided into A sublattice and B sublattice.

sets the internal index equal to the physical index so that $\alpha = 1$ represents a string and $\alpha = 0$ represents no string. The meaning of the tensor $T_{\alpha\beta\gamma\delta}$ is also clear: it just enforces the closed-string constraint, only allowing an even number of strings to meet at a vertex.

In this example, we have shown how to represent the simplest string-net condensed state using the TPS construction. We now explain how to extend this construction to the general case.

III. DOUBLE-SEMION MODEL

Let us start by turning to a slightly less straightforward model which illustrates some details necessary for our TPS construction for general string-net states. The model, which we call the double-semion model, is a spin-1/2 model where the spins are located on the links of the honeycomb lattice. The Hamiltonian is defined in Eq. (40) of Ref. 21. Here we will focus on the ground state which is known exactly. As in the previous example, the ground state can be described in the string language by interpreting the $\sigma^z = -1$ and $\sigma^z = 1$ states on a single link as the presence or absence of a string. The ground-state wave function is a superposition of closed-string states weighted by different phase factors

$$|\Psi_{d \text{ semion}}\rangle = \sum_{X \text{ closed}} (-)^{n(X)} |X\rangle, \quad (5)$$

where n is the number of closed loops in the closed-string state X .^{20,21} As in the previous example, this state contains nontrivial topological order. In this case, the state contains quasiparticle excitations with semion statistics.

Like the Z_2 state, the above string-net condensed state can be written as a TPS with one set of tensors T on the vertices and another set of tensors g on links. However, in this case it is more natural to use a rank-6 tensor T and a rank-5 tensor g . These tensors can be represented by double lines as in Fig. 2. The T tensors are given by

$$\text{sublattice A: } T_{\alpha\alpha';\beta\beta';\gamma\gamma'} = T_{\alpha\beta\gamma}^0 \delta_{\alpha'\beta'} \delta_{\beta'\gamma'} \delta_{\gamma'\alpha'},$$

$$\text{sublattice B: } T_{\alpha\alpha';\beta\beta';\gamma\gamma'} = T_{\alpha\beta\gamma}^0 \delta_{\alpha'\beta'} \delta_{\beta'\gamma'} \delta_{\gamma'\alpha'}, \quad (6)$$

where now each internal unphysical index α, β, \dots runs over 0, 1. Here, the tensor T^0 is given by

$$T_{\alpha\beta\gamma}^0 = \begin{cases} 1 & \text{if } \alpha + \beta + \gamma = 0, 3 \\ i & \text{if } \alpha + \beta + \gamma = 1 \\ -i & \text{if } \alpha + \beta + \gamma = 2. \end{cases} \quad (7)$$

The rank-5 g tensors are given by

$$g_{00,00}^\dagger = g_{11,11}^\dagger = 1, \quad g_{01,01}^\dagger = g_{10,10}^\dagger = 1, \quad \text{others} = 0. \quad (8)$$

Again, the ground-state wave function can be obtained by summing over all the internal indices on the connected links in the tensor network (see Fig. 2)

$$|\Psi_{d \text{ semion}}\rangle = \sum_{\{m_i\}} \text{tTr}[\otimes_v T \otimes g^{m_i}] |m_1, m_2, \dots\rangle. \quad (9)$$

From Eq. (8) we see that the physical indices and the internal indices have a simple relation: each pair of internal unphysical indices describes the presence/absence of string on the corresponding link. Two identical indices (00 and 11) in a pair correspond to no string (spin up) on the link and two opposite indices (01 and 10) in a pair correspond to a string (spin down) on the link. We may think of each half of the double line as belonging to an associated hexagon, and because every line along the edge of a hexagon takes the same value, we can assign that value to the hexagon. In this way we may view physical strings as domain walls in some fictitious Ising model as indicated by the coloring in Fig. 2. The peculiar assignment of phases in T^0 serves to guarantee the right sign oscillations essentially by counting the number of left and right turns made by the domain wall.

Equation (9) is interesting since the wave function (5) appears to be intrinsically nonlocal. We cannot determine the number of closed loops by examining a part of a string net. We have to examine how strings are connected in the whole graph. But such a “nonlocal” wave function can indeed be expressed as a TPS in terms of local tensors.

IV. GENERAL STRING-NET MODELS

We now show that the general string-net condensed states constructed in Ref. 21 can be written naturally as TPS. To this end, we quickly review the basic properties of the general string-net models and string-net condensed states.

The general string-net models are spin models where the spins live on the links of the honeycomb lattice. Each spin can be in $N+1$ states labeled by $a=0, 1, \dots, N$. The Hamiltonians for these models are exactly soluble and are defined in Eq. (11) of Ref. 21. Here, we focus on the (string-net condensed) ground states of these Hamiltonians.

In discussing these ground states it will be convenient to use the string picture. In this picture, we regard a link with a spin in state $a \neq 0$ as being occupied by a type- a string. We think of a link with $a=0$ as being empty. As in the previous examples, the ground states are superpositions of many different string configurations. However, in the more general case, the strings can branch (e.g., three strings can meet at a vertex).

To specify a particular string-net model or equivalently a particular string-net condensed state, one needs to provide certain data. First, one needs to specify an integer N —the number of string types. Second, one needs to give a rank-3 tensor δ_{abc} taking values 0, 1, where the indices a , b , and c range over $0, 1, \dots, N$. This tensor describes the branching rules: when $\delta_{abc}=0$, that means that the ground-state wave function does not include configurations in which strings a , b , and c meet at a point. On the other hand, if $\delta_{abc}=1$ then such branchings are allowed. Third, the strings can have an orientation and one needs to specify the string type a^* corresponding to a type- a string with the opposite orientation. A string is not oriented if $a=a^*$. Finally, one needs to specify a complex rank-6 tensor F_{klm}^{ijm} , where $i, j, k, l, m, n = 0, 1, \dots, N$. The tensor F_{klm}^{ijm} defines a set of local rules which implicitly define the wave function for the string-net condensed state. We would like to mention that the data $(N, \delta_{ijk}, F_{klm}^{ijm})$ cannot be specified arbitrarily. They must satisfy special algebraic relations in order to define a valid string-net condensed state.

The main fact that we will use in our construction of the TPS representation of general string-net condensed states is that the string-net condensed states can be constructed by applying local projectors B_p (p is a plaquette of the honeycomb lattice) to a no-string state $|0\rangle$.²¹ These projectors B_p can be written as

$$B_p = \sum_s a_s B_p^s, \quad (10)$$

where B_p^s has the simple physical meaning of adding a loop of type- s string around the hexagon p . The constants a_s are given by

$$a_s = \frac{d_s}{D}, \quad (11)$$

where $d_s = 1/F_{ss^*0}^{ss^*0}$ and $D = \sum_s d_s^2$.

This fact enables us to write the string-net condensed state as

$$\begin{aligned} |\Psi_{\text{string-net}}\rangle &= \prod_p B_p |0\rangle = \prod_p \sum_s a_s B_p^s |0\rangle \\ &= \sum_{u,s,t,\dots} a_t a_s a_u \dots |t,s,u,\dots\rangle_{\text{coh}}, \end{aligned} \quad (12)$$

where

$$|t,s,u,\dots\rangle_{\text{coh}} = B_{p_1}^t B_{p_2}^s B_{p_3}^u \dots |0\rangle. \quad (13)$$

Note that $[B_{p_1}^t, B_{p_2}^s] = 0$ when $p_1 \neq p_2$ and the order of the B_p^s operators in the above is not important.

These states are not orthogonal to each other. In the following, we would like to express these states in terms of the orthonormal basis of different string-net configurations

$$|t,s,u,\dots\rangle_{\text{coh}} = \sum_{i,j,k,\dots} \Phi_{i,j,k,\dots}^{t,s,u,\dots} |i,j,k,\dots\rangle. \quad (14)$$

Here $|i,j,k,\dots\rangle$ is a string-net configuration and $i,j,k,\dots = 0, \dots, N$ label the string types (i.e., the physical states) on the corresponding link [see Fig. 3(c)]. We note that

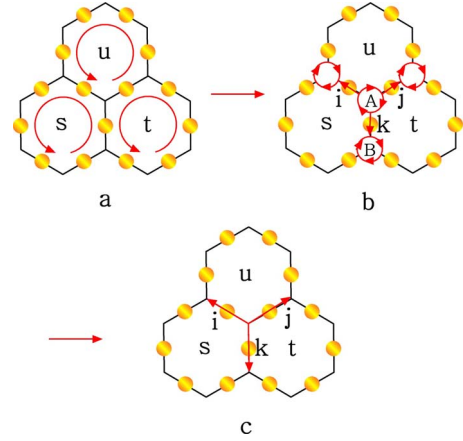


FIG. 3. (Color online) Using the fusion rules, we can represent the coherent states $|t,s,u,\dots\rangle$ in terms of the orthogonal string-net states.

$t,s,u,\dots = 0, \dots, N$ label the string types associated with the hexagons [see Fig. 3(a)]. As a result, the string-net condensed state is given by

$$|\Psi_{\text{string-net}}\rangle = \sum_{t,s,u,\dots} a_t a_s a_u \dots \sum_{i,j,k,\dots} \Phi_{i,j,k,\dots}^{t,s,u,\dots} |i,j,k,\dots\rangle.$$

To calculate $\Phi_{i,j,k,\dots}^{t,s,u,\dots}$, we note that the coherent states $|t,s,u,\dots\rangle_{\text{coh}}$ can be viewed as string-net state in a fattened lattice [see Fig. 3(a)].²¹ To obtain the string-net states where strings live on the links, we need to combine the two strings looping around two adjacent hexagons into a single string on the link shared by the two hexagons. This can be achieved by using the string-net recoupling rules²¹ (see Fig. 3). This allows us to show that the string-net condensed state can be written as (see Appendix A)

$$|\Psi_{\text{string-net}}\rangle = \sum_{t,s,u,\dots} \left[\prod_{\text{hexagon}} a_t \right] \sum_{i,j,k,\dots} \left[\prod_{\text{vert}} \sqrt{v_i v_j v_k} G_{tsu}^{ijk} \right] |i,j,k,\dots\rangle, \quad (15)$$

where $G_{tsu}^{ijk} \equiv F_{ts^*u}^{ijk} / (v_k v_u)$ is the symmetric $6j$ symbol with full tetrahedral symmetry³⁵ and $v_i = \sqrt{d_i}$.

Let us explain the above expression in more detail. The indices i,j,k,\dots are on the links while the indices u,t,s,\dots are on the hexagons. Each hexagon contributes to a factor a_s . Each vertex in A sublattice contributes to a factor $\sqrt{v_i v_j v_k} G_{tsu}^{ijk}$.

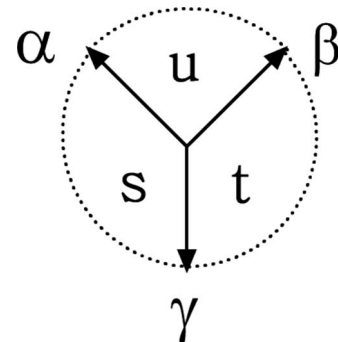


FIG. 4. The graphic representation for the tensor $G_{tsu}^{\alpha\beta\gamma}$.

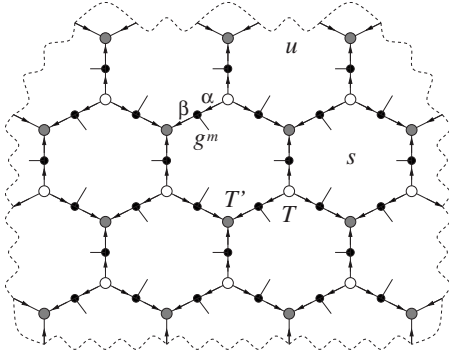


FIG. 5. A tensor complex formed by vertices, links, and faces. The dashed curves are boundaries of the faces. The links that connect the dots carry index α, β, \dots and the faces carry index u, s, \dots . Each trivalent vertex represents a T tensor. The vertices on A sublattice (open dots) represent $T_{\alpha\beta\gamma;tsu}$. The vertices on B sublattice (shaded dots) represent $T'_{\alpha\beta\gamma;tsu} = T_{\alpha^*\beta^*\gamma^*;tsu}$. The dots on the links represent the g^m tensor $g_{\alpha,\beta}^m$. In the weighted tensor trace, the α, β, \dots indices on the links that connect the dots are summed over, and the u, s, \dots indices on the closed faces are summed over with a weighting factor $a_u a_s, \dots$.

and each vertex in B sublattice contributes to a factor $\sqrt{v_i v_j v_k} G_{tsu}^{i^* j^* k^*}$. The indices i, j, k, t, s , and u around a vertex are arranged as illustrated in Fig. 4.

Expression (15) can be formally written as a weighted tensor trace over a tensor complex formed by T tensors and g^m tensors. First, let us explain what a tensor complex is. A tensor complex is formed by vertices, links, and faces (see Fig. 5). T tensors live on the vertices and g^m tensors live on the links. The T tensor carries the indices from the three connected links and the three adjacent faces, while the g^m tensor carries the indices from the two connected links (see Fig. 6). By having indices on faces, the tensor complex generalizes the tensor network.

The weighted tensor trace sums over all the α, β, \dots indices on the internal links that connect two dots and sums over all the u, s, \dots indices on the internal faces that are enclosed by the links, with weighting factors a_u, a_s , etc. from each enclosed face. Let us choose the T tensors on vertices to be (see Fig. 7)

$$\begin{aligned} \text{A sublattice: } T_{\alpha\beta\gamma;tsu} &= \sqrt{v_\alpha v_\beta v_\gamma} G_{tsu}^{\alpha\beta\gamma}, \\ \text{B sublattice: } T'_{\alpha\beta\gamma;tsu} &= \sqrt{v_\alpha v_\beta v_\gamma} G_{tsu}^{\alpha^*\beta^*\gamma^*}, \end{aligned} \quad (16)$$

and the g^m tensor to be

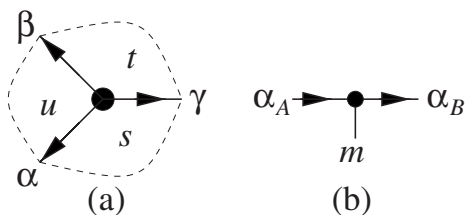


FIG. 6. The graphic representation of (a) the T tensor, $T_{\alpha\beta\gamma;tsu}$, and (b) the g^m tensor $g_{\alpha_A\alpha_B}^m$.

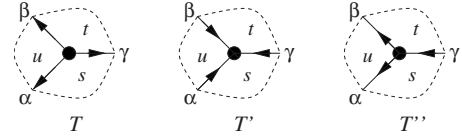


FIG. 7. Three T tensors associated with different orientations of the legs are related: $T_{\alpha\beta\gamma;tsu}$, $T'_{\alpha\beta\gamma;tsu} = T_{\alpha^*\beta^*\gamma^*;tsu}$, and $T''_{\alpha\beta\gamma;tsu} = T_{\alpha\beta\gamma^*;tsu}$.

$$g_{\alpha_A\alpha_B}^m = \delta_{\alpha_A m} \delta_{\alpha_B m}. \quad (17)$$

In this case the string-net condensed state (15) can be written as a weighted tensor trace over a tensor complex

$$|\Psi_{\text{strnet}}\rangle = \sum_{m_1, m_2, \dots} \text{wt Tr}[\otimes_v T \otimes_l g^{m_l}] |m_1, m_2, \dots\rangle, \quad (18)$$

where m_i label the physical states on the links. We note that the g^m tensor is just a projector: it makes each edge of the hexagon to have the same index that is equal to m . The string-net condensed state (15) can also be written as a more standard tensor trace over a tensor network (see Appendix B).

The string-net states and the corresponding TPS representation can also be generalized to arbitrary trivalent graph in two dimensions. After a similar calculation as that on the honeycomb lattice, we find that an expression similar to Eq. (15) describes the string-net condensed state on a generic trivalent graph in two dimensions [see Fig. 8(a)]. The indices in Eq. (15), such as i, j, k, u, s, t, \dots , should be read from the Fig. 8(a), where the indices of the G symbol is determined by three oriented legs and three faces between them (see Fig. 4).

Such a string-net wave function can be expressed in terms of weighted tensor trace over a tensor complex [see Fig. 8(b)]

$$|\Psi_{\text{strnet}}\rangle = \sum_{m_1, m_2, \dots} \text{wt Tr}[\otimes_v T \otimes_l g^{m_l}] |m_1, m_2, \dots\rangle, \quad (19)$$

where the T tensors, depending on the orientations on the legs, are given by Figs. 7 and 16.

V. STRING-NET WAVE FUNCTION AS A FIXED-POINT WAVE FUNCTION

An interesting property of the string-net condensed states

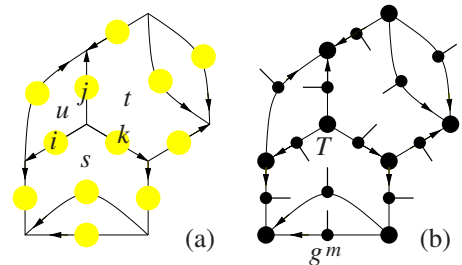


FIG. 8. (Color online) (a) The string-net condensed states on arbitrary trivalent graph in two dimensions can be written as (b) a weighted tensor trace over a tensor complex formed by T and g^m tensors.

constructed in Ref. 21 is that they have a vanishing correlation length: $\xi=0$. This suggests that the string-net condensed states are fixed points of some kind of renormalization-group transformation.²¹ In this section, we attempt to make this proposal concrete. We show that the string-net condensed

states are fixed points of the TERG introduced in Ref. 32. To understand and motivate the TERG, it is useful to first think about the problem of computing the norm and local-density matrix of the string-net state (19). To obtain the norm, we note that

$$\begin{aligned} \text{coh}\langle u_2, s_2, t_2, \dots | u_1, s_1, t_1, \dots \rangle_{\text{coh}} &= \sum_{i,j,k,\dots} \sum_{i',j',k',\dots} \dots F_{s_1^* s_1^* i}^{u_1^* u_1^* 0} F_{u_1^* u_1^* j}^{t_1^* t_1^* 0} F_{t_1^* t_1^* k}^{s_1^* s_1^* 0} \\ &\times (F_{s_2^* s_2^* i'}^{u_2^* u_2^* 0} F_{u_2^* u_2^* j'}^{t_2^* t_2^* 0} F_{t_2^* t_2^* k'}^{s_2^* s_2^* 0})^* \dots \langle X_b' | X_b \rangle = \sum_{i,j,k,\dots} \left[\prod_{\text{vertices}} \frac{v_i v_j v_k}{v_{t_1} v_{s_1} v_{u_1} v_{t_2} v_{s_2} v_{u_2}} F_{t_1^* s_1^* u_1}^{ijk} (F_{t_2^* s_2^* u_2}^{ijk})^* \right] \\ &\times \frac{v_{s_1} v_{t_1} v_{s_2} v_{t_2}}{v_k v_k} = \sum_{i,j,k,\dots} \left[\prod_{\text{vertices}} v_i v_j v_k G_{t_1^* s_1^* u_1}^{ijk} G_{u_2^* s_2^* t_2}^{k^* j^* i^*} \right]. \end{aligned} \quad (20)$$

Thus, the norm can be written as

$$\begin{aligned} \langle \Psi_{\text{stnet}} | \Psi_{\text{stnet}} \rangle &= \sum_{i,j,k,\dots} \sum_{t_1, s_1, u_1, \dots} \sum_{t_2, s_2, u_2, \dots} \left[\prod_{\text{hexagon}} a_{t_1} a_{t_2} \right] \\ &\times \left[\prod_{\text{vertices}} v_i v_j v_k G_{t_1^* s_1^* u_1}^{ijk} G_{u_2^* s_2^* t_2}^{k^* j^* i^*} \right] \\ &= \text{wt Tr}[\mathbb{T} \otimes \mathbb{T} \otimes \mathbb{T} \otimes \dots], \end{aligned} \quad (21)$$

where we have used the identity $(F_{tsu}^{ijk})^* = F_{ust}^{k^* j^* i^*} \frac{v_k v_u}{v_i v_j}$. Here wt Tr is a tensor trace over a tensor complex formed by the double-tensor \mathbb{T} (see Fig. 9). Again, the tensor complex are formed by vertices, links, and faces. Each trivalent

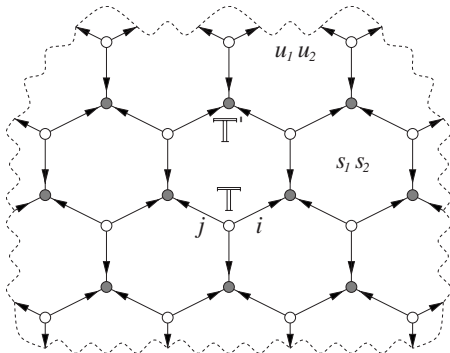


FIG. 9. A tensor complex with vertices, links, and faces is formed by the double tensors \mathbb{T} and \mathbb{T}' . (Dashed curves are boundaries of the faces.) The links that connect the dots carry index i, j, \dots and the faces carry double-index $u_1 u_2, s_1 s_2, \dots$. Each trivalent vertex represents a double- \mathbb{T} tensor. The vertices on A sublattice (open dots) represents $\mathbb{T}_{ijk;t_1 t_2, s_1 s_2, u_1 u_2}$. The vertices on B sublattice (shaded dots) represents $\mathbb{T}'_{ijk;t_1 t_2, s_1 s_2, u_1 u_2} = \mathbb{T}_{i^* j^* k^*; t_1 t_2, s_1 s_2, u_1 u_2}$. In the weighted tensor trace, the i, j, \dots indices on the links that connect the dots are summed over and the $u_1 u_2, s_1 s_2, \dots$ indices on the closed faces are summed over independently with a weighting factor $a_{u_1} a_{u_2} a_{s_1} a_{s_2}, \dots$

vertex on the $A(B)$ sublattice represent a double tensor $\mathbb{T}(\mathbb{T}')$,

$$\begin{aligned} \text{A: } \mathbb{T}_{ijk; s_1 s_2, t_1 t_2, u_1 u_2} &= v_i v_j v_k G_{t_1^* s_1^* u_1}^{ijk} G_{u_2^* s_2^* t_2}^{k^* j^* i^*}, \\ \text{B: } \mathbb{T}'_{ijk; s_1 s_2, t_1 t_2, u_1 u_2} &= v_i v_j v_k G_{t_1^* s_1^* u_1}^{i^* j^* k^*} G_{u_2^* s_2^* t_2}^{k j i}. \end{aligned} \quad (22)$$

The double-tensor \mathbb{T} can be represented by a graph with three oriented legs and three faces between them (see in Fig. 10) where each leg or face now carries two indices. In wt Tr, we sum over all indices on the internal links. We also sum over all indices on the internal faces independently with weighting factors $a_{u_1} a_{u_2}$ from each of the internal faces.

With minor modification, this expression for the norm can be used to compute expectation values for local operators. Indeed, the local-density matrix is given by a similar tensor trace, except that the physical indices i, j, k, \dots need to be left unsummed in the region where we want to compute the den-

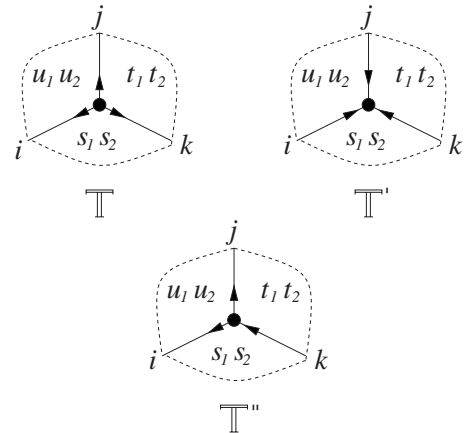


FIG. 10. Graphic representations for the three double- \mathbb{T} tensors $\mathbb{T}_{ijk;t_1 t_2, s_1 s_2, u_1 u_2}$, $\mathbb{T}'_{ijk;t_1 t_2, s_1 s_2, u_1 u_2} = \mathbb{T}_{i^* j^* k^*; t_1 t_2, s_1 s_2, u_1 u_2}$, and $\mathbb{T}''_{ijk;t_1 t_2, s_1 s_2, u_1 u_2} = \mathbb{T}_{ijk^*; t_1 t_2, s_1 s_2, u_1 u_2}$.

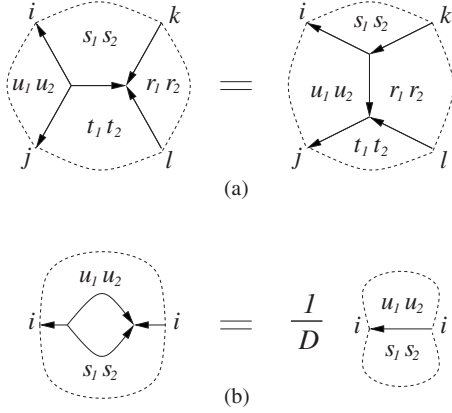


FIG. 11. Graphic representation of the basic rules for the double tensor \mathbb{T} : (a) the deformation rule and (b) the reduction rule.

sity matrix. Thus, the problem of computing expectation values and norms can be reduced to the problem of evaluating the tensor trace (21).

Unfortunately, evaluating tensor traces is an exponentially hard problem in two or higher dimensions. This leads us to the TERG method. The idea of the TERG method is to (approximately) evaluate tensor traces by coarse graining.³⁶ In each coarse-graining step, the tensor complex G with tensor \mathbb{T} is reduced to a smaller complex \tilde{G} with tensor $\tilde{\mathbb{T}}$. Repeating this operation many times allows one to evaluate tensor traces of arbitrarily large complexes. One can therefore compute expectation values of TPS with relatively little effort.

In general, the coarse-graining transformation is implemented in an approximate way. That is, one finds a tensor $\tilde{\mathbb{T}}$ such that $\text{wt Tr}[\mathbb{T} \otimes \mathbb{T} \otimes \dots]_G \approx \text{wt Tr}[\tilde{\mathbb{T}} \otimes \tilde{\mathbb{T}} \otimes \dots]_{\tilde{G}}$. However, as we show below, it can be implemented *exactly* in the case of the string-net condensed states. Moreover, $\tilde{\mathbb{T}} = \mathbb{T}$, so that the string-net condensed states are fixed points of the TERG transformation.

To see this, note that the double- \mathbb{T} tensor has the following special properties (see Appendix C for a derivation).

Basic rule 1. The deformation rule of \mathbb{T} ,

$$\begin{aligned} \sum_m \mathbb{T}_{m,j,i;u_1,s_1,t_1;u_2,s_2,t_2} \mathbb{T}_{m^*,k^*,l^*;r_1,t_1,s_1;r_2,t_2,s_2} \\ = \sum_m \mathbb{T}_{m,i,k^*;s_1,r_1,u_1;s_2,r_2,u_2} \mathbb{T}_{m^*,l^*,j^*;t_1,u_1,r_1;t_2,u_2,r_2}. \end{aligned} \quad (23)$$

Basic rule 2. The reduction rule of \mathbb{T} ,

$$\begin{aligned} \sum_{m,l,t_1,t_2} a_{t_1} a_{t_2} \mathbb{T}_{i,l,m;t_1,s_1,u_1;t_2,s_2,u_2} \mathbb{T}_{m^*,l^*,j^*;u_1,s_1,t_1;u_2,s_2,t_2} \\ = \frac{1}{D} \delta_{ij} \delta_{s_2^* u_2} \delta_{s_1^* i u_1}. \end{aligned} \quad (24)$$

The above two basic rules can be represented graphically as in Fig. 11(a) and 12. The two basic rules also lead to another useful property of the double- \mathbb{T} tensor as represented by Fig. 12.

The relations in Figs. 11(a) allow us to reduce the tensor complex that represents the norm of the string-net condensed

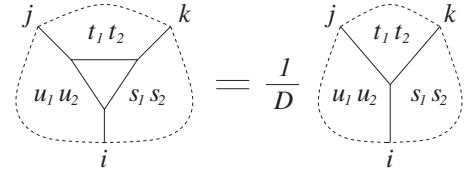


FIG. 12. A useful reduction of tensor complex.

state to a coarse-grained tensor complex of the same shape (see Fig. 13). This coarse-graining transformation is exactly the TERG transformation. Since the tensor \mathbb{T} is invariant under such a transformation, we see that the string-net wave function is a fixed point of the TERG transformation.

VI. CONCLUSIONS AND DISCUSSIONS

In conclusion, we found a TPS representation for all the string-net condensed states. The local tensors are analogous to local order parameters in Landau's symmetry broken theory. As an application of TPS representation, we presented the TERG transformation and show that the TPSs obtained from the string-net condensed states are fixed points of the TERG transformation. In Ref. 32, we have shown that all the physical measurements, such average energy of a local Hamiltonian, correlation functions, etc. can be calculated very efficiently by using the TERG algorithm under the TPS representations. Thus, TPS representations and TERG algorithm can capture the long-range entanglements in topologically ordered states. They may be an effective method and a powerful way to study quantum phases and quantum phase transitions between different topological orders.

Recently, it has come to our attention that the connection between the triple-line tensor network and the string-net states is also discussed independently in a related paper by Buerschaper, Aguado, and Vidal (Ref. 37).

ACKNOWLEDGMENTS

This research is supported by the Foundational Questions Institute (FQXi) and NSF under Grant No. DMR-0706078.

APPENDIX A: TENSOR PRODUCT STATE FROM STRING-NET RECOUPLING RULE

To calculate $\Phi_{i,j,k,\dots}^{u,s,t,\dots}$, we note that the coherent states $|u,s,t,\dots\rangle_{\text{coh}}$ can be viewed in a string-net state in a fattened lattice [see Fig. 3(a)].²¹ To obtain the string-net states where strings live on the links, we need to combine the two strings looping around two adjacent hexagons into a single string on the link shared by the two hexagons. We make use of the

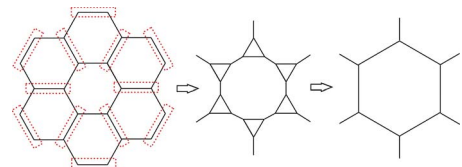


FIG. 13. (Color online) The coarse-graining procedure for honeycomb lattice.

string-net recoupling rules²¹ (see Fig. 3) to represent the coherent states $|u, s, t, \dots\rangle_{\text{coh}}$ in terms of proper orthogonal string states

$$|u, s, t, \dots\rangle_{\text{coh}} = \sum_{i, j, k, \dots} \dots F_{s^* s i}^{u^* u 0} F_{u^* u j}^{t^* t 0} F_{t^* t k}^{s^* s 0} \dots |X_b\rangle,$$

where X_b is the string-net state described in Fig. 3(b). Note that on each link we have a factor such as $F_{s^* s i}^{u^* u 0}$ and we multiply such kind of factors on all links together. Using $F_{s^* s i}^{u^* u 0} = \frac{v_i}{v_s v_u} \delta_{us^* i}$, we can rewrite the above as

$$|u, s, t, \dots\rangle_{\text{coh}} = \sum_{i, j, k, \dots} \dots \frac{v_i}{v_s v_u} \delta_{us^* i} \frac{v_j}{v_t v_u} \delta_{tu^* j} \frac{v_k}{v_s v_t} \delta_{st^* k} \dots |X_b\rangle. \quad (\text{A1})$$

Applying the string-net recoupling rules again, we rewrite the above as

$$|u, s, t, \dots\rangle_{\text{coh}} = \sum_{i, j, k, \dots} \prod_{\text{vertices}} \frac{\sqrt{v_i v_j v_k}}{v_t v_s v_u} F_{ts^* u}^{ijk} |i, j, k, \dots\rangle \frac{v_s v_t}{v_k}, \quad (\text{A2})$$

$$= \sum_{i, j, k, \dots} \prod_{\text{vertices}} \sqrt{v_i v_j v_k} G_{tsu}^{ijk} |i, j, k, \dots\rangle, \quad (\text{A3})$$

where $G_{tsu}^{ijk} = F_{ts^* u}^{ijk} / v_k v_u$ is the symmetric 6j symbol with full tetrahedral symmetry. Putting Eq. (A3) into Eq. (12), we finally obtain

$$|\Psi_{\text{stnet}}\rangle = \sum_{i, j, k, \dots} \sum_{t, s, u, \dots} \left[\prod_{\text{hexagon}} a_t \right] \left[\prod_{\text{vertices}} \sqrt{v_i v_j v_k} G_{tsu}^{ijk} \right] \times |i, j, k, \dots\rangle. \quad (\text{A4})$$

We note that the indices, such as i, j, k, u, s, t, \dots , should be read from the Fig. 3. The arrow in (out) on a vertex will determine that we put k^* or k in the G symbol. In this convention, the physical labels in the G symbol are always valued as k^* on sublattice A (arrow in) and k on sublattice B (arrow out).

APPENDIX B: STRING-NET CONDENSED STATE AS A TPS ON A TENSOR NETWORK

We have expressed the string-net condensed state (15) as a weighted tensor trace on the tensor complex. In this section, we will show that the string-net condensed state (15) can also be written as a more standard tensor trace over a tensor network

$$|\Psi_{\text{stnet}}\rangle = \sum_{m_1, m_2, \dots} \text{tTr}[\otimes_v T \otimes_l g^m] |m_1, m_2, \dots\rangle. \quad (\text{B1})$$

Here the tensor network (see Fig. 14) is formed by two kinds of tensors: a T tensor for each vertex and a g^m tensor for each link. Unlike the tensors in Fig. 2, now T and g^m have a triple-line structure (see Fig. 15). The T tensor on a vertex is given by

$$T_{u' au; t' \beta t; s' \gamma s} = T_{\alpha \beta \gamma; tsu}^0 \delta_{ut'} \delta_{ts'} \delta_{su'}, \quad (\text{B2})$$

where

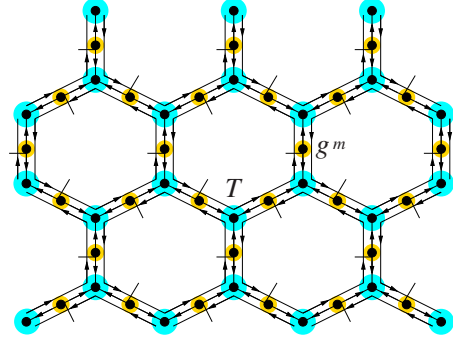


FIG. 14. (Color online) A tensor network where each tensor has triple-line structure. The tensor trace sums over all the indices on the links that connect two dots.

$$T_{\alpha \beta \gamma; tsu}^0 = (a_t a_s a_u)^{1/6} \sqrt{v_\alpha v_\beta v_\gamma} G_{tsu}^{\alpha \beta \gamma}. \quad (\text{B3})$$

As shown in Fig. 4, T^0 can be labeled by three oriented lines and three faces between them. Notice that $T_{\alpha \beta \gamma; tsu}^0$ has the cyclic symmetry $T_{\alpha \beta \gamma; tsu}^0 = T_{\beta \gamma \alpha; sut}^0 = T_{\gamma \alpha \beta; uts}^0$ due to the tetrahedron symmetry of G symbol.

The g^m tensor on each link is a projector

$$g_{u'_A \alpha_A u_A; u'_B \alpha_B u_B}^m = h_{\alpha_A \alpha_B; u_A u_B}^m \delta_{u_A u'_B} \delta_{u_B u'_A}, \quad (\text{B4})$$

$$h_{\alpha_A \alpha_B; u_A u_B}^m = \delta_{\alpha_A m} \delta_{\alpha_B m},$$

where m is the physical index running from 0 to N and represents the $N+1$ different string types (plus the no-string state). Note that u_A, α_A , and u'_A are indices on the side of the A sublattice and u_B, α_B , and u'_B are indices on the side of the B sublattice. Basically, g^m makes $m = \alpha_A$ and $\alpha_A = \alpha_B$. The corresponding edge of the hexagon has a string of type m . The choice of $\delta_{\alpha_A \alpha_B}$ in g^m makes the T tensors to be the same on the A and B sublattices.

Our construction has a slightly different form from the usual TPS construction, but we can bring our construction into the usual form with a single set of tensors $T^{(M)}$ defined on vertices. This is because the matrix g^m on each link is basically a projector (with a twist), so that we can always split it into two matrices g^{mA} and g^{mB} (see Fig. 16) and associate one with each vertex the link touches. Doing this for every link in effect displaces the physical degrees of freedom from the links to the vertices. This procedure seems to enlarge the Hilbert space on each link from H_m to $H_{m_A} \otimes H_{m_B}$,

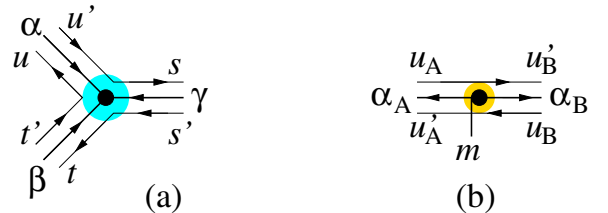


FIG. 15. (Color online) (a) The T tensor, $T_{u' au; t' \beta t; s' \gamma s} = T_{\alpha \beta \gamma; tsu}^0 \delta_{ut'} \delta_{ts'} \delta_{su'}$, and (b) the g^m tensor $g_{u'_A \alpha_A u_A; u'_B \alpha_B u_B}^m = h_{\alpha_A \alpha_B; u_A u_B}^m \delta_{u_A u'_B} \delta_{u_B u'_A}$, with a triple-line structure.

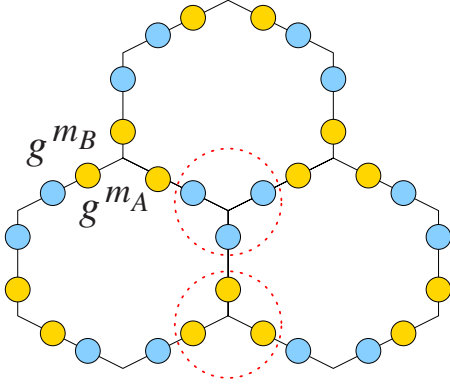


FIG. 16. (Color online) The T - g from TPS representations for string-net states can be deformed to standard TPS representations by splitting the matrix g^m into two matrices g^{m_A} , g^{m_B} on each link and recombining three sites around a vertex (the three states inside a dashed circle) into one site.

however, the operators g^{m_A} and g^{m_B} impose the constraint $m_A = m_B$ keeping the physical Hilbert space intact. Grouping the displaced physical degrees of freedom on each vertex into a new physical variable M we can combine three sites around each vertex into one site. This is illustrated in Fig. 16, where the states in each dashed circle are labeled by M . With this slight reworking of the degrees of freedom, the new tensors on sublattices A and B can be expressed as

$$\begin{aligned} T_{A, ucau'; t\beta t'; s\gamma s'}^{iA j_A k_A} &= T_{\alpha\beta\gamma; tsu}^{0iA j_A k_A} \delta_{ut'} \delta_{ts'} \delta_{su'} \delta_{\alpha i_A} \delta_{\beta j_A} \delta_{\gamma k_A}, \\ T_{B, ucau'; t\beta t'; s\gamma s'}^{k_B l_B m_B} &= T_{\alpha^* \beta^* \gamma^*; t' s' u'}^{0k_B l_B m_B} \delta_{u't} \delta_{t's} \delta_{s'u} \delta_{\alpha^* k_B} \delta_{\beta^* l_B} \delta_{\gamma^* m_B}, \end{aligned} \quad (\text{B5})$$

with

$$T_{\alpha\beta\gamma; tsu}^{0ijk} = (a_i a_s a_u)^{1/6} \sqrt{v_i v_j v_k} G_{tsu}^{\alpha\beta\gamma}, \quad (\text{B6})$$

where ijk are physical indices M . Note that the tensors $T_A^{iA j_A k_A}$ and $T_B^{k_B l_B m_B}$ still have a triple-line structure. The string-net condensed state now can be rewritten as

$$|\Psi_{\text{string-net}}\rangle = \sum_{M_1, M_2, \dots} \text{tTr}_{\otimes} T_{A(B)}^{M} |M_1, M_2, \dots\rangle. \quad (\text{B7})$$

APPENDIX C: PROOF OF BASIC RULES OF T

The two basic rules can be proved easily by using the pentagon identity.²¹ First, the pentagon identity leads to a decomposition law for supertensor \mathbb{T}

$$\begin{aligned} \mathbb{T}_{i,j,k;t_1,s_1,u_1;t_2,s_2,u_2} &= v_i v_j v_k G_{t_1 s_1 u_1}^{ijk} G_{u_2 s_2 t_2}^{k^* j^* i^*} \\ &= v_i v_j v_k \sum_n d_n G_{s_1 u_1 n}^{u_2 s_2^* i} G_{u_1 t_1 n}^{t_2 u_2^* j} G_{t_1 s_1 n}^{s_2 t_2^* k}. \end{aligned}$$

Using this expression, it is easy to proof the two basic rules, Eqs. (23) and (24). Here we also use the symmetries of G symbol

$$G_{tsu}^{ijk} = G_{uts}^{kij} = G_{ij^* u^*}^{ts^* k^*}, \quad (\text{C1})$$

which can be easily verified from the symmetry of F symbol

$$F_{ts^* u}^{ijk} = F_{ut^* s}^{kij} \frac{v_k v_u}{v_j v_s} = F_{iju^*}^{ts^* k^*} \quad (\text{C2})$$

and the definition of G symbol.

Then let us proof the deformation rule Eq. (23). Proof:

$$\begin{aligned} \sum_m \mathbb{T}_{m,j,i;u_1,s_1,t_1;u_2,s_2,t_2} \mathbb{T}_{m^*,k^*,l^*;r_1,t_1,s_1;r_2,t_2,s_2} &= v_i v_j v_k v_l \sum_{n,n',m} d_n d_{n'} d_m G_{s_1 t_1 n}^{t_2 s_2^* m} G_{t_1 u_1 n}^{u_2 t_2^* j} G_{u_1 s_1 n}^{s_2 u_2^* i} G_{t_1 s_1 n'}^{s_2 t_2^* m^*} G_{s_1 r_1 n'}^{r_2 s_2^* k^*} G_{r_1 t_1 n'}^{t_2 r_2^* l^*} \\ &= v_i v_j v_k v_l \sum_{n,n'} d_n d_{n'} \left(\sum_m d_m G_{s_1 t_1 n}^{t_2 s_2^* m} G_{t_1 s_1 n'}^{s_2 t_2^* m^*} \right) G_{t_1 u_1 n}^{u_2 t_2^* j} G_{u_1 s_1 n}^{s_2 u_2^* i} G_{s_1 r_1 n'}^{r_2 s_2^* k^*} G_{r_1 t_1 n'}^{t_2 r_2^* l^*} \\ &= v_i v_j v_k v_l \sum_{n,n'} d_n d_{n'} \left(\sum_m d_m G_{t_2^* s_2^* m}^{s_1 t_2^* n} G_{t_1^* s_1^* m}^{s_2 t_1^* n} \right) G_{t_1 u_1 n}^{u_2 t_2^* j} G_{u_1 s_1 n}^{s_2 u_2^* i} G_{s_1 r_1 n'}^{r_2 s_2^* k^*} G_{r_1 t_1 n'}^{t_2 r_2^* l^*} \\ &= v_i v_j v_k v_l \sum_n d_n G_{t_1 u_1 n}^{u_2 t_2^* j} G_{u_1 s_1 n}^{s_2 u_2^* i} G_{s_1 r_1 n}^{r_2 s_2^* k^*} G_{r_1 t_1 n}^{t_2 r_2^* l^*}. \end{aligned} \quad (\text{C3})$$

In the last step we use the simple pentagon identity²¹

$$\sum_m d_m G_{t_2^* s_2^* m}^{s_1 t_2^* n} G_{t_1^* s_1^* m}^{s_2 t_1^* n} = \frac{\delta_{nn'}}{d_n} \delta_{s_1^* s_2^* n} \delta_{t_1^* t_2^* n}. \quad (\text{C4})$$

Similarly, we have

$$\begin{aligned} \sum_m \mathbb{T}_{m,i,k^*;s_1,r_1,u_1;s_2,r_2,u_2} \mathbb{T}_{m^*,j^*;t_1,u_1,r_1;t_2,u_2,r_2} &= v_i v_j v_k v_l \sum_n d_n G_{u_1 s_1 n}^{s_2 u_2^* i} G_{s_1 r_1 n}^{r_2 s_2^* k^*} G_{r_1 t_1 n}^{t_2 r_2^* j^*} G_{t_1 u_1 n}^{u_2 t_2^* l^*} \end{aligned}$$

Finally, we have

$$\sum_m \mathbb{T}_{m,j,i;u_1,s_1,t_1;u_2,s_2,t_2} \mathbb{T}_{m^*,k^*,l^*;r_1,t_1,s_1;r_2,t_2,s_2} = \sum_m \mathbb{T}_{m,i,k^*;s_1,r_1,u_1;s_2,r_2,u_2} \mathbb{T}_{m^*,l^*;j;t_1,u_1,r_1;t_2,u_2,r_2}. \quad (\text{C5})$$

The reduction rule is also easy to proof by using pentagon identity.²¹ Proof:

$$\begin{aligned} \sum_{m,l,t_1,t_2} a_{t_1} a_{t_2} \mathbb{T}_{i,l,m;t_1,s_1,u_1;t_2,s_2,u_2} \mathbb{T}_{m^*,l^*,j^*;u_1,s_1,t_1;u_2,s_2,t_2} &= v_i v_j \sum_{n,n',m,l,t_1,t_2} d_n d_{n'} d_m d_l a_{t_1} a_{t_2} G_{s_1 u_1 n}^{u_2 s_2 i} G_{u_1 t_1 n}^{t_2 u_2 l} G_{t_1 s_1 n}^{s_2 t_2 m} G_{s_1 t_1 n'}^{t_2 s_2 m^*} G_{t_1 u_1 n'}^{u_2 t_2 l^*} G_{u_1 s_1 n'}^{s_2 u_2 j^*} \\ &= v_i v_j \sum_{n,n',t_1,t_2} d_n d_{n'} a_{t_1} a_{t_2} G_{s_1 u_1 n}^{u_2 s_2 i} G_{u_1 s_1 n'}^{s_2 u_2 j^*} \left(\sum_l d_l G_{u_1 t_1 n}^{t_2 u_2 l} G_{t_1 u_1 n'}^{u_2 t_2 l^*} \right) \left(\sum_m d_m G_{t_1 s_1 n}^{s_2 t_2 m} G_{s_1 t_1 n'}^{t_2 s_2 m^*} \right) \\ &= v_i v_j \sum_{n,t_1,t_2} \delta_{t_1 t_2 n}^* a_{t_1} a_{t_2} G_{s_1 u_1 n}^{u_2 s_2 i} G_{u_1 s_1 n}^{s_2 u_2 j^*} = v_i v_j \sum_n a_n G_{s_1 u_1 n}^{u_2 s_2 i} G_{u_1 s_1 n}^{s_2 u_2 j^*} \\ &= \frac{v_i v_j}{D} \sum_n d_n G_{s_1 u_1 n}^{u_2 s_2 i} G_{u_1 s_1 n}^{s_2 u_2 j^*} = \frac{1}{D} \delta_{ij} \delta_{s_2 i u_2}^* \delta_{s_1 i u_1}^*. \end{aligned} \quad (\text{C6})$$

Notice in the third line, we use the fact that $a_{t_2} = a_2^*$.

-
- ¹L. D. Landau, Phys. Z. Sowjetunion **11**, 26 (1937).
²D. C. Tsui, H. L. Stormer, and A. C. Gossard, Phys. Rev. Lett. **48**, 1559 (1982).
³X.-G. Wen, Int. J. Mod. Phys. B **4**, 239 (1990).
⁴X.-G. Wen and Y.-S. Wu, Phys. Rev. Lett. **70**, 1501 (1993).
⁵T. Senthil, J. B. Marston, and M. P. A. Fisher, Phys. Rev. B **60**, 4245 (1999).
⁶X.-G. Wen, Phys. Rev. Lett. **84**, 3950 (2000).
⁷X.-G. Wen, Phys. Rev. B **65**, 165113 (2002).
⁸T. Senthil, L. Balents, S. Sachdev, A. Vishwanath, and M. P. A. Fisher, Phys. Rev. B **70**, 144407 (2004).
⁹T. Senthil, Science **303**, 1490 (2004).
¹⁰N. Read and S. Sachdev, Phys. Rev. Lett. **66**, 1773 (1991).
¹¹X.-G. Wen, Phys. Rev. B **44**, 2664 (1991).
¹²T. Senthil and M. P. A. Fisher, Phys. Rev. B **62**, 7850 (2000).
¹³R. Moessner and S. L. Sondhi, Phys. Rev. Lett. **86**, 1881 (2001).
¹⁴S. Sachdev and K. Park, Ann. Phys. (N.Y.) **298**, 58 (2002).
¹⁵G. Misguich, D. Serban, and V. Pasquier, Phys. Rev. Lett. **89**, 137202 (2002).
¹⁶L. Balents, M. P. A. Fisher, and S. M. Girvin, Phys. Rev. B **65**, 224412 (2002).
¹⁷X.-G. Wen, Phys. Rev. Lett. **90**, 016803 (2003).
¹⁸A. Y. Kitaev, Ann. Phys. (N.Y.) **303**, 2 (2003).
¹⁹L. B. Ioffe, M. V. Feigel'man, A. Ioselevich, D. Ivanov, M. Troyer, and G. Blatter, Nature (London) **415**, 503 (2002).
²⁰M. Freedman, C. Nayak, K. Shtengel, K. Walker, and Z. Wang, Ann. Phys. (N.Y.) **310**, 428 (2004).
²¹M. A. Levin and X. G. Wen, Phys. Rev. B **71**, 045110 (2005).
²²M. A. Levin and X.-G. Wen, Rev. Mod. Phys. **77**, 871 (2005).
²³A. Kitaev and J. Preskill, Phys. Rev. Lett. **96**, 110404 (2006).
²⁴M. Levin and X.-G. Wen, Phys. Rev. Lett. **96**, 110405 (2006).
²⁵F. Verstraete and J. I. Cirac, arXiv:cond-mat/0407066 (unpublished).
²⁶G. Vidal, Phys. Rev. Lett. **99**, 220405 (2007).
²⁷M. Aguado and G. Vidal, Phys. Rev. Lett. **100**, 070404 (2008).
²⁸A. Klumper, A. Schadschneider, and J. Zittartz, J. Phys. A **24**, L955 (1991).
²⁹D. Perez-Garcia, F. Verstraete, M. Wolf, and J. Cirac, Quantum Inf. Comput. **7**, 401 (2007).
³⁰S. R. White, Phys. Rev. Lett. **69**, 2863 (1992).
³¹X.-G. Wen, Phys. Lett. A **300**, 175 (2002).
³²Z.-C. Gu, M. Levin, and X.-G. Wen, Phys. Rev. B **78**, 205116 (2008).
³³R. Koenig, B. W. Reichardt, and G. Vidal, arXiv:0806.4583 (unpublished).
³⁴F. Verstraete, M. M. Wolf, D. Perez-Garcia, and J. I. Cirac, Phys. Rev. Lett. **96**, 220601 (2006).
³⁵Such a G_{isu}^{ijk} is slightly different from that introduced in Ref. **21**.
³⁶M. Levin and C. P. Nave, Phys. Rev. Lett. **99**, 120601 (2007).
³⁷O. Buerschaper, M. Aguado, and G. Vidal, following paper, Phys. Rev. B **79**, 085119 (2009).